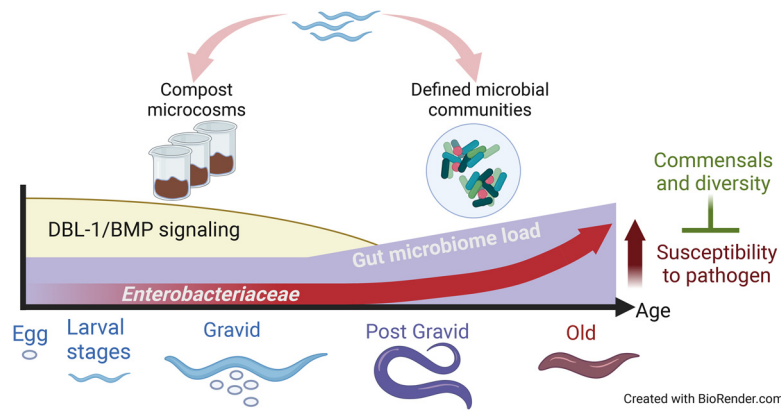


An *Enterobacteriaceae* Bloom in Aging Animals is Restrained by the Gut Microbiome



Authors

Rebecca Choi, Rahul Bodkhe, Barbara Pees, Dan Kim, Maureen Berg, David Monnin, Juhyun Cho, Vivek Narayan, Ethan Deller, Cathy Savage-Dunn, and Michael Shapira

Correspondence

mshapira@berkeley.edu

Research Paper

An *Enterobacteriaceae* Bloom in Aging Animals is Restrained by the Gut Microbiome

Rebecca Choi,¹ Rahul Bodkhe,¹ Barbara Pees,¹ Dan Kim,¹ Maureen Berg,¹ David Monnin,¹ Juhyun Cho,¹ Vivek Narayan,¹ Ethan Deller,¹ Cathy Savage-Dunn,² and Michael Shapira^{1,*}

¹Department of Integrative Biology, University of California, Berkeley, Berkeley, CA, USA

²Department of Biology, Queens College, City University of New York, Flushing, NY, USA

*Corresponding author: mshapira@berkeley.edu

<https://doi.org/10.59368/agingbio.20240024>

The gut microbiome plays important roles in host function and health. Core microbiomes have been described for different species, and imbalances in their composition, known as dysbiosis, are associated with pathology. Changes in the gut microbiome and dysbiosis are common in aging, possibly due to multi-tissue deterioration, which includes metabolic shifts, dysregulated immunity, and disrupted epithelial barriers. However, the characteristics of these changes, as reported in different studies, are varied and sometimes conflicting. Using clonal populations of *Caenorhabditis elegans* to highlight trends shared among individuals, we employed 16S rRNA gene sequencing, colony-forming unit counts, and fluorescent imaging, identifying an *Enterobacteriaceae* bloom as a common denominator in aging animals. Experiments using *Enterobacter hormaechei*, a representative commensal, suggested that the *Enterobacteriaceae* bloom was facilitated by a decline in Sma/BMP immune signaling in aging animals and demonstrated its potential for exacerbating infection susceptibility. However, such detrimental effects were context-dependent and mitigated by competition with commensal communities, highlighting the latter as determinants of healthy versus unhealthy aging, depending on their ability to restrain opportunistic pathobionts.

Introduction

Aging is a process of multi-tissue deterioration, including muscular atrophy, neurodegeneration, epithelial barrier disruption, immune dysregulation, and metabolic remodeling. Vulnerabilities and pathologies associated with this deterioration directly impact lifespan. In the case of the intestine, age-dependent impairments (immune, barrier, and metabolic) further converge to alter the niche that is home to a complex community of microbes, the gut microbiome. However, how such changes affect the gut microbiome is not well understood.

The gut microbiome is increasingly appreciated for its contributions to host function^{1–4}. Imbalances in composition, or dysbiosis, have been shown to play a causative role in pathology (e.g., obesity)^{5,6}. Age-dependent dysbiosis was described in flies, mice, and humans and was suggested to negatively impact both barrier functions and immune fitness^{7–9}. Studies in human populations have shown that the microbiomes of healthy octogenarians differed from those of unhealthy individuals of similar age¹⁰. Other studies characterized the trajectory of microbiome changes through aging all the way to semi-supercentenarian (105–110 years old)¹¹, offering further insights into the relationship between age-dependent changes in microbiome composition and host health. Importantly, transplanting microbiomes from young mice to old reduced markers of aging and ameliorated health^{12,13}, and a similar transfer in killifish increased lifespan¹⁴, demonstrating a causal role for age-dependent changes in microbiome composition in host aging. However, for the most part,

such studies could not identify common trends in age-dependent changes that may offer points for intervention to ameliorate pathologies. Perhaps the sole exception is the identification of increased abundance of *Proteobacteria* (now renamed *Pseudomonadota*) in aging animals, both in vertebrates, where they are a minor constituent of the gut microbiome of young individuals, and in invertebrates, where they comprise a larger part in young animals and further increase with age^{7,15–17}. However, the significance of this bloom and whether it is a universal signature of the aging gut microbiome are yet to be determined.

The nematode *Caenorhabditis elegans*, a useful model for aging research, is now gaining momentum as a model for microbiome research. It offers the advantage of working with synchronized, initially germ-free, clonal populations, which overcome the limitations of interindividual variation common to vertebrate models to better discern shared patterns in microbiome composition¹⁸. As a bacterivore, *C. elegans* ingests bacteria from its environment. While some bacteria are digested as food, others persist, giving rise to a characteristic gut microbiome, similar across populations raised in the lab in different environments or in worms isolated from different geographical locations, yet distinct from the respective microbial environments^{19–21}. As in other organisms, gut commensals were shown to provide diverse benefits to their host, including faster development and resistance to pathogens^{20–24}. The power of *C. elegans* as a genetic model further enabled identification of some of the genes, many of which are immune regulators^{25–27}, that help control commensals and their function and shape microbiome composition.

We used *C. elegans* to characterize changes in gut microbiome composition during aging, identifying a bloom in bacteria of the *Enterobacteriaceae* family that was associated with an age-dependent decline in immune DBL-1/BMP signaling. The *Enterobacteriaceae* bloom was found to be potentially harmful, increasing vulnerability to infection. However, competing commensals, or a diverse microbiome, were able to mitigate these detrimental effects. The results presented highlight an *Enterobacteriaceae* bloom as a hallmark of normal aging and suggest that the outcomes of this bloom are context-dependent, determined by the ability of the rest of the gut microbiome to restrain it, distinguishing between healthy and non-healthy aging.

Materials and Methods

Worm strains

C. elegans strains included wildtype (WT) N2, *dbl-1(nk3)*, and the *dbl-1* overexpressing strain BW1940, obtained from the *Caenorhabditis* Genome Center (CGC); transgenic strains expressing green fluorescent protein (GFP) from the *spp-9* promoter, TLG690, *texIs127[spp-9p::GFP]*, TLG707, *texIs127;dbl-1(nk3)* and TLG708, *texIs127;texIs100[dbl-1p::GFP::dbl-1]*, were gratefully received from Tina Gumienny^{28,29} and *eat-2(ad1116)* mutants were gratefully received from Andrew Dillin. Gain-of-function (gof) *sma-4(syb2546)* mutants were generated using CRISPR/Cas9 editing to insert a GFP tag at the N-terminus of the endogenous *sma-4* locus. C-terminal tags disrupt function by blocking Smad complex formation^{30,31}. GFP::SMA-4 animals display gof phenotypes such as long body size (measured in images using ImageJ), presumably due to loss of autoinhibition mediated by interaction between N-terminal MH1 and C-terminal MH2 domains³².

Bacterial strains and communities

Escherichia coli strain OP50 and the gram-positive pathogen *Enterococcus faecalis* strain V583 were obtained from the CGC. Two defined communities of worm gut commensals were used: CeMbio, with twelve strains, represents the worm core gut microbiome³³ and SC20, a subset of 20 strains of the previously described SC1²⁵, with eight species out of the 20 of the *Enterobacteriaceae* family (Table 1). In addition, a subset of CeMbio strains was used in experiments testing effects on susceptibility to *Enterococcus faecalis* infection, including only strains that are sensitive to gentamycin, which is used in *E. faecalis* plates, to prevent enrichment of gut commensals through the environment. Additional commensals of the genus *Pantoea*, family *Erwiniaceae* (a recent splinter off *Enterobacteriaceae*), included BIGb0393 (also in CeMbio) and the recently characterized *Pantoea cyripedii* strains V8 and T16²³.

Bacterial communities were prepared for experiments by growing individual strains in lysogeny broth (LB) at 28 °C for two days, adjusting cultures to 1 OD, concentrating 10-fold, and mixing equal volumes from each culture. 100–200 µL aliquots of the mix were plated on either minimal nematode growth medium (NGM) or peptone-free medium (PFM), which further limits bacterial growth³³, as described, and air-dried for 2–12 hours prior to the addition of worms.

Construction of fluorescently tagged *Enterobacter hormaechei* CEent1-dsRed

E. hormaechei CEent1, previously misidentified as *E. cloacae*²², is a member of both the CeMbio and SC20 communities. The construction of its dsRed-expressing derivative was achieved by integrating the *dsRed* gene into the functionally neutral *attTn7*

Table 1. SC20 members.

Strain name	Family	Genus	Species
CEent1-dsRed	<i>Enterobacteriaceae</i>	<i>Enterobacter</i>	<i>hormaechei</i>
MSPm1	<i>Pseudomonadaceae</i>	<i>Pseudomonas</i>	<i>Berkeleyensis</i>
Cre-5.2	<i>Enterobacteriaceae</i>	<i>Enterobacter</i>	NA
L3-3L	<i>Sphingobacteriaceae</i>	<i>Sphingobacterium</i>	<i>puteale</i>
oak-5.2	<i>Enterobacteriaceae</i>	<i>Buttiauxella</i>	NA
CEent3-GFP	<i>Enterobacteriaceae</i>	<i>Enterobacter</i>	<i>ludwigii</i>
WG-2.2	<i>Pseudomonadaceae</i>	<i>Pseudomonas</i>	<i>plecoglossicida</i>
WG-2.4	<i>Micrococcaceae</i>	<i>Arthrobacter</i>	NA
WG-2.5	<i>Microbacteriaceae</i>	<i>Microbacterium</i>	<i>barkeri</i>
2.1	<i>Bacillaceae</i>	<i>Bacillus</i>	<i>nealsonii</i>
3.1	<i>Bacillaceae</i>	<i>Bacillus</i>	<i>asahii</i>
3.2	<i>Bacillaceae</i>	<i>Bacillus</i>	<i>megaterium</i>
10.1	<i>Bacillaceae</i>	<i>Lysinibacillus</i>	<i>pakistanensis</i>
10.3	<i>Bacillaceae</i>	<i>Lysinibacillus</i>	<i>pakistanensis</i>
14.1	<i>Bacillaceae</i>	<i>Bacillus</i>	<i>subtilis</i>
19.1.7	<i>Bacillaceae</i>	<i>Lysinibacillus</i>	<i>fusiformis</i>
19.3.3	<i>Enterobacteriaceae</i>	<i>Rahnella</i>	<i>victoriana</i>
19.3.8	<i>Enterobacteriaceae</i>	<i>Buttiauxella</i>	<i>agrestis</i>
CBent2	<i>Enterobacteriaceae</i>	<i>Lelliottia</i>	<i>amnigena</i>
Cbent1	<i>Enterobacteriaceae</i>	<i>Citrobacter</i>	<i>freundii</i>

site in the CEent1 genome using the site-specific Tn7-mini transposon system³⁴ (Supplementary Fig. 1). Transposon insertion was achieved through triparental mating with a donor strain and a transposase-expressing helper strain, both based on the diaminopimelic acid (DAP)-auxotrophic and *pir1*-positive *E. coli* strain BW29427, containing the conjugative RP4 mating system as a chromosomal insert. This strain, as well as other *E. coli* strains and plasmids used in constructing the fluorescently-tagged strains, were gratefully received from the Goodrich-Blair lab, University of Tennessee Knoxville. Briefly, the original *GFP* in the mini-transposon, carried on plasmid pURR25 (Supplementary Fig. 1), was replaced with *dsRed* by digesting the plasmid with BseRI and NheI to cleave out the *GFP* coding sequence³⁵, amplifying the *dsRed* gene from pBK-miniTn7-ΩGm-DsRed³⁶ using primers 5'-TAC GTG CAA GCA GAT TAC GG-3' and 5'-ATC CAG TGA TTT TTT TCT CCAT-3', and ligating the amplified *dsRed* to the linearized pURR25 vector. The modified pURR25 plasmid, carrying the *pir1*-dependent *oriR6K* as well as *dsRed* and the antibiotic resistance genes *KanR* and *StrR*, was reintroduced by electroporation into its original host strain, constituting the donor strain. The transposase plasmid, pUX-BF13, in the helper strain also included the *pir1*-dependent *oriR6K* and *AmpR* antibiotic resistance, along with the *Tn7*-transposase³⁷.

Recipient strain CEent1 (*pir1*-negative), donor, and helper strains were each cultured until they reached an OD₆₀₀ of 0.4 and then mixed in a 1:1:1 ratio in SOC DAP media for one hour at 37 °C. The mixture was spread on LB DAP plates for an additional 24-hour incubation to promote conjugation. Bacteria subsequently underwent several rounds of re-streaking on Kan⁺/DAP⁻ plates to select for integrant CEent1 cells and to dilute out the *pir1*-negative plasmids which cannot be replicated in CEent1 (Supplementary Fig. 1). Integrant clones were verified as CEent1 by sequencing a 200-bp fragment of the CEent1 gene for *gyrB* using the primers 5'-GCA AGC AGG AAC AGT ACA TT-3' and 5'-TCG GCT GAT AAA TCA GCT CTT TC-3'.

Microcosm experiments

Compost microcosms harboring diverse microbial communities were prepared from local soil composted with produce for up to two weeks, essentially as previously described^{19,38}. Briefly, local soils were supplemented with banana peels or chopped apples. The composted soils were split into two parts: one (6 g in a glass vial) autoclaved to eliminate native nematodes, and the other (10 g of soil) suspended in M9 buffer to obtain a microbial extract which was concentrated and added to the autoclaved samples to reconstitute the original microbial community.

Synchronized worm populations were prepared by bleaching gravid worms and releasing eggs that hatched in M9 salt solution to provide germ-free L1 larvae. In continuous aging experiments, synchronized populations of germ-free L1 worms were raised at 20 °C in separate vials containing the same compost and harvested at advancing ages up to day five of adulthood (D5) (Fig. 1A). The final time point was determined by the need to distinguish between the original cohort (post-reproductive, or post-gravid, at D5) and progeny (mid-stage gravids), which could not be achieved in subsequent time points. In experiments with fixed-time colonization, worms were raised on live *E. coli* until the L4 stage to ensure proper development, then transferred to kanamycin-killed *E. coli*³⁹, from which worms were further transferred at advancing ages to microcosm environments for two days before harvesting for analysis. For the earliest time point (gravids, day zero of adulthood), worms spent only 4 hours on dead *E. coli*

before transferring to microcosms. This was deemed necessary to minimize the carryover of live *E. coli*, which can colonize older worms. A two-day exposure time was selected for all worm populations as it is the time required to obtain well-colonized worms in microcosms initiated with L1 larvae, used for the earliest time point. Worm harvesting was carried out using a Baermann funnel, as described in ref.³⁸.

Soil samples (1 g) were taken from microcosms of the same compost batch used to grow worms ("soil") or from the same microcosm from which worms were harvested ("grazed soil").

Experiments with defined bacterial communities

Aging experiments on bacterial communities/strains were carried out similarly to the description for microcosm experiments, with bacteria seeded on NGM or PFM plates as described. In continuous aging experiments, worms were transferred to fresh plates every day during the reproductive phase to separate the original cohort from their progeny, enabling carrying on experiments into later stages of adulthood.

DNA extraction

Worms harvested in microcosm experiments (100–500 per group, except for the last time point of the continuous aging experiment in which only eight post-gravid worms could be retrieved) were extensively washed, surface-sterilized by letting them crawl for an hour on plates with 100 µg/mL gentamycin, and used for DNA extraction with the QIAGEN PowerSoil DNA isolation kit (Cat. #12888) as previously described²⁵.

Worms harvested from plates with defined communities (100–150 per group) were washed three times with M9, paralyzed with 25 mM levamisole (Acros Organics) to close their intestine, and surface-sterilized with 2% bleach in M9, as described in ref.³⁸. DNA was extracted using the DNeasy PowerSoil Pro Kit (Qiagen Cat. #47016) according to manufacturer instructions, with the following modification: to break open worms prior to the first step of the protocol, worms were incubated in the kit's buffer for 10 min at 60 °C, then crushed with added zirconium beads using a PowerLyzer (2000 RPM 2 × 30 sec).

16S rRNA gene sequencing and analysis

DNA samples from worms and their respective environments were used to generate sequencing libraries for the 16S V4 region. Libraries from microcosms experiments were prepared using tailed primers, as previously described¹⁹, and sent for 150 paired-end sequencing to the UC Davis sequencing facility. Analysis of bacterial 16S amplicon data was carried out using the QIIME2 software pipeline⁴⁰. Sequence reads were demultiplexed and filtered for quality control, with 85.6% of all reads passing quality filtering, providing an average read of 121,053 reads per sample. Sequences were aligned and clustered into operational taxonomic units (OTU) based on the closed reference OTU picking algorithm using the QIIME2 implementation of UCLUST⁴¹, and the taxonomy of each OTU was assigned based on 99% similarity to reference sequences based on Greengenes release 13.8. Prior to diversity analysis, all communities were rarefied to 116,543 sequences per sample. Shannon's diversity and Faith's phylogenetic diversity were calculated to assess the *alpha* diversity of soil and worm gut microbiotas^{42,43}. Shannon diversity is a composite measure of both richness and evenness, while the Faith method takes the phylogenetic distance of species into account. Weighted UniFrac distances were calculated to assess

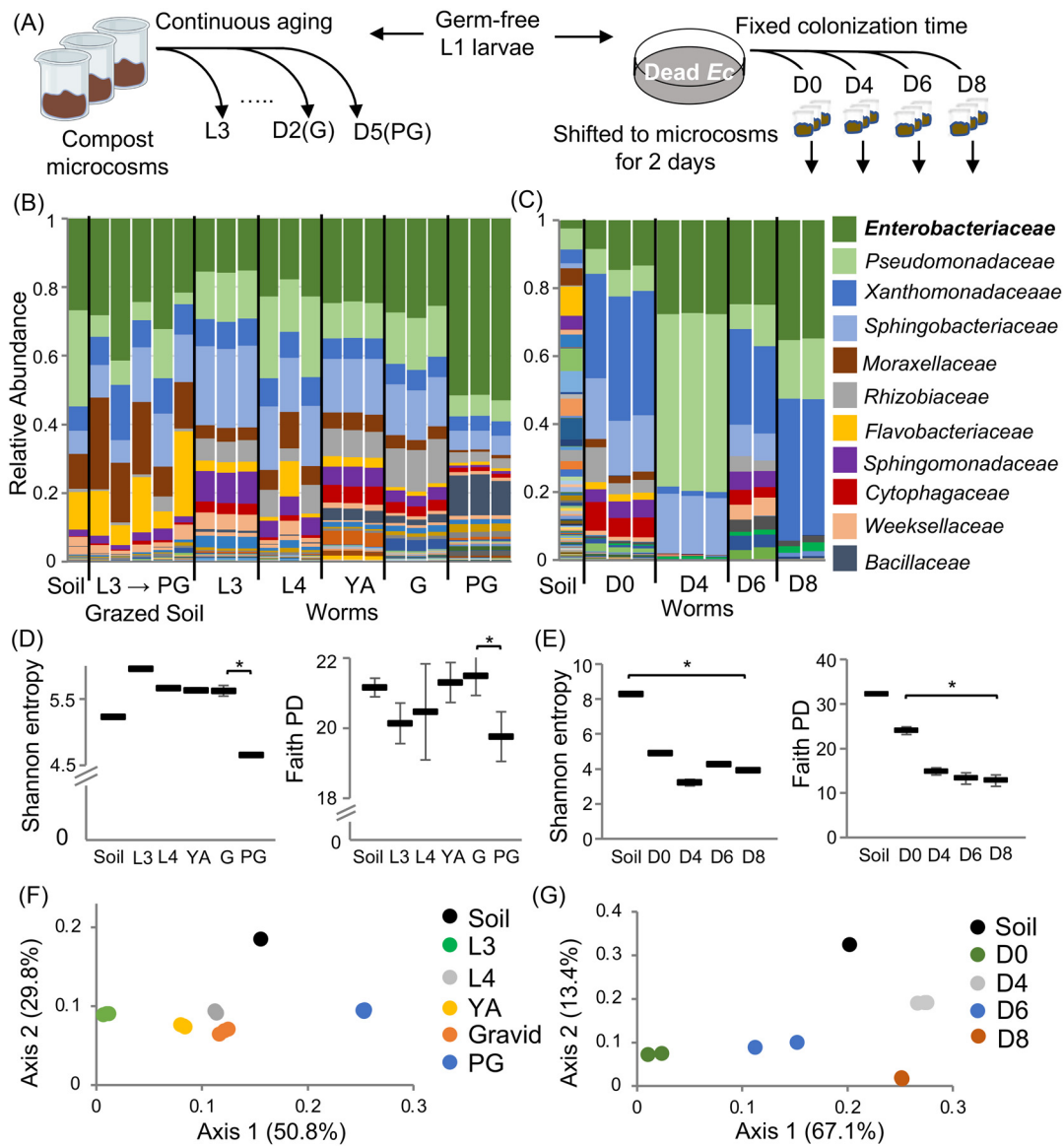


Figure 1. Gut *Enterobacteriaceae* bloom in worms aging in natural-like environments. (A) Two sampling schemes for worm microbiome analysis during late development and early aging. Dead *Ec* stands for dead *E. coli*. 16S rRNA gene sequencing of microbiome composition (B) in worms raised continuously in microcosm environments or (C) in worms of advancing ages, shifted for two days to microcosm environments. Bars represent microbiomes in microcosm environments or in the gut of worms raised in these microcosms (each bar represents a population of 100 worms). Taxa are shown at family-level resolution. B, L3, and L4, larval stages; YA, young adults; G, gravid (D2, second day of adulthood); PG, post-gravid (D5). C and D0, early gravids. (D,E) Alpha diversity represented by Shannon and Faith phylogeny indices; *, $p < 0.05$, t test. (F,G) Principal coordinate analysis based on weighted UniFrac distances between microbiomes.

beta diversity and used in principal coordinate analysis (PCoA). Raw data and metadata can be accessed at <https://www.ncbi.nlm.nih.gov/sra> with accession number PRJNA982115.

Fluorescence imaging

For each time point examined, 30–40 worms were picked off CEent1-dsRed, or CEent3-GFP-containing plates (with the single strain or with the fluorescent strains as part of a community), washed with M9, paralyzed with 10 mM Levamisole, and mounted on a slide with a 2%–4% agarose pad. Imaging was performed with a Leica MZ16F equipped with a QImaging MicroPublisher 5.0 camera. The quantification of fluorescent signals was conducted using the Fiji plugin within the ImageJ

package v2.10/1.53c or 1.53f51⁴⁴. Integrated density values were measured per worm after subtracting background mean gray values and autofluorescence and normalizing for worm area.

Quantifying bacterial load by colony-forming unit (CFU) counting

For each time point examined, 10–15 worms were washed three times in M9-T (M9/0.0125% TritonX-100), paralyzed with 25 mM Levamisole, and surface sterilized by a three-minute incubation in 2% bleach³³. After two washes of 1 mL of PBS-T (PBS/0.0125% Triton-X 100), worms were collected in a final volume of 100 μ L. Samples of the final wash were plated and incubated at 28 °C for two days to verify the removal of external bacteria.

To release bacteria from the worm gut, worms were crushed with 10–15 zirconium beads in 100 μ L of PBS in a PowerLyzer at 4000 RPM for 30–45 sec. Released bacteria were diluted and plated either on nonselective LB agar plates (for all bacteria) or *Enterobacteriaceae*-selective Violet Red Bile Glucose (VRBG) plates. CFUs were counted after 1–2 days of incubation at 28 °C. CFUs for *E. hormaechei* and *Lelliottia amnigena* could be distinguished on VRBG plates based on morphology.

Quantifying bacterial load via quantitative PCR (qPCR)

When CFU counts on selective VRBG medium could not offer the required resolution between *Enterobacteriaceae* and other bacteria, relative bacterial load was measured with real-time qPCR using the eubacterial 16S rRNA gene primers 806f (5'-AGATACCCCGGTAGTC-3') and 895r (5'-CYGYACTCCCAGGYG-3') and the *Enterobacteriaceae*-specific 16S specific primers Ent_MB_F (5'-ACCTGAGCGTCAGTCTTTGTC-3') and R (5'-GTAGCGGTGA AATGCGTAGAGA-3')²⁵. qPCR was performed using Bio-Rad SsoAdvanced Universal SYBR Green qPCR Supermix and an Applied Biosystems StepOne Plus real-time PCR system. Cycling (eubacterial primers): 95 °C for 5 min, 45 \times [95 °C for 15 sec, 60 °C for 30 sec, 72 °C for 15 sec], 72 °C for 5 min; and for the *Enterobacteriaceae*-specific primers: 95 °C for 5 min, 40 \times [95 °C for 15 sec, 60 °C for 30 sec], 72 °C for 5 min.

Ct values for bacterial 16S were normalized to worm material by subtracting Ct values obtained for worm actin using the pan-actin primers^{45,46}.

Survival assays

For infection resistance experiments, synchronized worm populations were raised from L1 on PFM plates with *E. coli* OP50, CEent1, or designated communities and shifted, at L4, or at day 4 of adulthood, to *E. faecalis* plates prepared with Brain Heart Infusion Agar containing 25 μ g/mL gentamicin and seeded with bacteria a day before the transfer of worms. *E. faecalis* strain V583 was previously shown to proliferate in the worm gut, killing adult worms within four days⁴⁷. Raising worms on CEent1 until L4 before shifting to pathogens allows for worm colonization while maintaining previously described infection parameters to facilitate comparisons^{22,47}. Assays were carried out at 25 °C, and dead or live worms were counted every day⁴⁸. For lifespan assays, worms were raised on designated strains or communities in PFM plates at 20 °C and scored daily for survival beginning at L4 (t_0).

Statistical analyses

Statistical tests were conducted in R (v. 3.6.3). Survival curves were statistically compared using Kaplan-Meier analysis and log-rank tests using the survdiff R package⁴⁹, and all graphs were created with the ggplot R package⁵⁰.

Results

C. elegans aging involves an expansion of bacteria in the *Enterobacteriaceae* family

To characterize changes in gut microbiome composition during *C. elegans* aging, worms were raised in fifteen identical natural-like microcosm environments, harvested at designated time points, three populations at a time, and analyzed using 16S rRNA gene sequencing (Fig. 1A, continuous aging). For each time point, the environmental compost microbiome of one of the three

samples was similarly analyzed. As previously observed, worm gut microbiomes were distinct from their environment (Fig. 1B)¹⁹. Furthermore, worm microbiomes changed with age, but these changes appeared to be independent of the availability of bacteria in the environment, where the microbial community remained largely unaltered during the experiment (Fig. 1B, grazed soil). Most prominently, we observed an expansion in gut *Enterobacteriaceae*, particularly in post-reproductive worms (post-gravid, day five of adulthood). This increase could be due to ecological succession inside the gut, shaped by interbacterial interactions; alternatively, it could be determined by age-dependent changes in the host and in the gut niche, directly affecting gut bacteria. To distinguish between the two possibilities, we carried out microcosm experiments where worms were raised on dead *E. coli* (i.e., fed but not colonized) and shifted to the complex microcosm community at advancing ages for a fixed amount of time, preventing age-associated differences attributed to ecological succession over accumulating time (Fig. 1A, right). While the initial soil microbiome in this experiment showed relatively higher microbial diversity compared to the experiment described in Figure 1B, the *Enterobacteriaceae* expansion re-emerged, suggesting that this expansion was associated with age-dependent changes in the intestinal niche rather than with the time of exposure and highlighting it as a potential hallmark of worm aging (Fig. 1C).

Gut bacterial diversity (alpha diversity) decreases during aging, which was more pronounced in the fixed-colonization-time aging experiment (Fig. 1E) but was also seen in post-gravid worms in the continuous aging experiment (Fig. 1D). Declines were observed in worm microbiome diversity both with respect to species richness and evenness, represented by the Shannon Index, as well as with respect to phylogenetic diversity, represented by the Faith Index (Fig. 1D,E). In addition, worm gut microbiomes of different ages differed from one another. PCoA based on weighted UniFrac distances showed that in both experiments, worms of a specific age harbored similar gut microbiomes, which were distinct from worm microbiomes in other ages, similar to trends observed in aging mice (Fig. 1F,G)⁵¹. Together, these results support a role for the age-modified intestinal niche in driving age-dependent changes in microbiome composition, including a prominent expansion of *Enterobacteriaceae* as well as a general decline in bacterial diversity.

An *Enterobacteriaceae* expansion is a recurring theme in worms aging in different microbial environments

Microcosm experiments provide natural-like microbial diversity. However, to investigate the *Enterobacteriaceae* bloom in greater detail, we turned to defined communities of characterized gut commensals. Two communities were used, each representing a slightly different paradigm: the publicly available CeMbio community, which includes two *Enterobacteriaceae* strains, *Enterobacter hormaechei* (CEent1) and *Lelliottia amnigena* (JUB66), but in the worm gut is dominated by *Stenotrophomonas* and *Ochrobactrum*³³, and SC20, which has a higher proportion of *Enterobacteriaceae* (8 out of 20 species), including CEent1 (Table 1). We used a CEent1-dsRed derivative included in both communities to enable imaging of gut colonization. In both, colonization with CEent1-dsRed increased with age, in line with the *Enterobacteriaceae* bloom observed in natural-like microcosm experiments (Fig. 2A,C). To examine whether the age-dependent bloom was specific to gut *Enterobacteriaceae* or also involved increases in

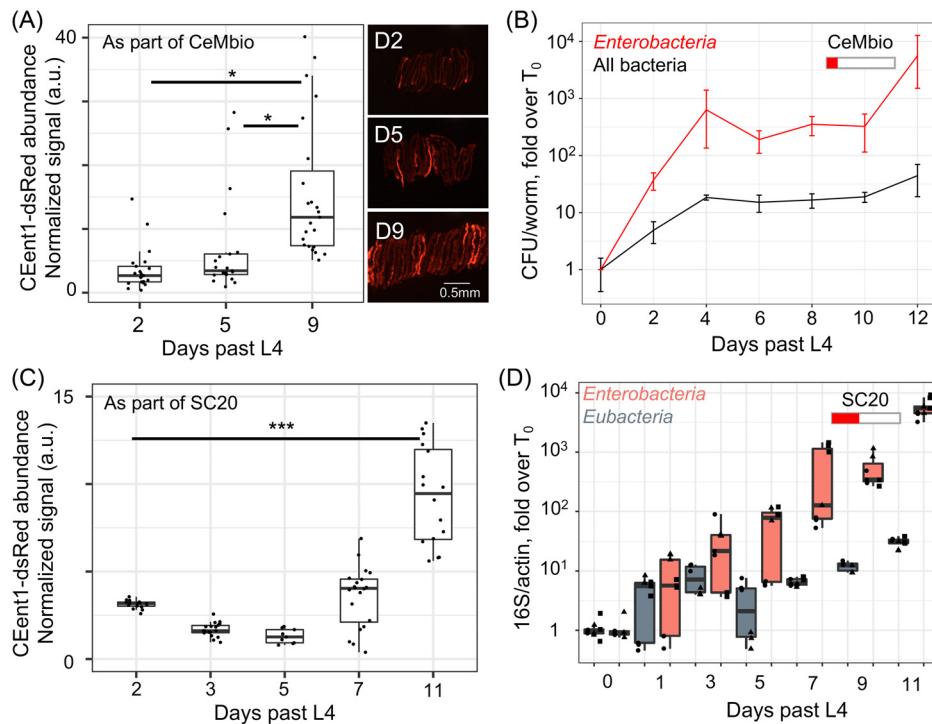


Figure 2. *Enterobacteriaceae* bloom is a common denominator of aging worms raised in different microbial environments. (A) Colonization of individual aging worms raised on CeMbio with CEent1-dsRed, $n = 21\text{--}23$ /group; $p < 0.01$, pairwise t tests. (B) Bacterial load in aging worms raised on CeMbio, based on colony-forming unit counts of *Enterobacteriaceae* on Violet Red Bile Glucose plates and of total bacteria on lysogeny broth plates. Shown are averages \pm standard deviations (SDs) for three plates per time point ($n = 4\text{--}12$ worms/time point). The bar with red coloration in panels (B) and (D) indicates the fraction of *Enterobacteriaceae* in the designated communities. (C) CEent1 colonization in aging worms raised on SC20 with CEent1-dsRed ($n = 9\text{--}18$ worms/time point); $p < 0.001$, pairwise t tests. (D) Fold change in bacterial load in worms aging on SC20, assessing bacterial load with quantitative PCR (qPCR) using primers specific for *Enterobacteriaceae* 16S or Eubacterial 16S, normalized to worm DNA assessed by qPCR with primers specific for *C. elegans* actin (shapes represent replicate plates, each evaluated by qPCR in duplicate or triplicate).

the abundance of other members of the gut microbiome, we used CFU counts and qPCR to evaluate gut bacterial load. In worms aging on CeMbio, an increase in total bacterial load (CFUs on non-selective LB) was observed, from 10^3 bacterial cells/worm at D0 (L4 larvae) to around 10^5 cells/worm at D12 of adulthood, a roughly 100-fold increase (Fig. 2B). However, a steeper increase was observed in the *Enterobacteriaceae* load (CFUs on selective VRBG plates), from being barely detectable at day 0 to about 5% of the total gut microbiome by old age (~ 5000 cells/worm), close to a 10^4 -fold increase. A similar trend was observed in worms raised on the *Enterobacteriaceae*-rich SC20 community, as demonstrated with qPCR using universal *Eubacteria* primers or *Enterobacteriaceae*-specific primers and normalized to worm DNA (represented by actin genes). This evaluation showed a much steeper increase in *Enterobacteriaceae* strains compared to the increase in the total bacterial load (Fig. 2D). These results support the notion that an *Enterobacteriaceae* bloom is a hallmark of aging, regardless of the initial conditions, such as high or low environmental diversity or a high or low initial proportion of *Enterobacteriaceae*. This bloom involves a large increase in total bacterial load but a proportionally larger increase in the *Enterobacteriaceae* load per worm.

An *Enterobacteriaceae* bloom in aging animals can have detrimental consequences

Previous work showed that the gut commensal CEent1, a representative *Enterobacteriaceae*, protected young animals from infection with the intestine-proliferating pathogen *Enterococcus*

faecalis^{22,48}. However, in worms disrupted for DBL-1/BMP immune signaling, gut abundance of CEent1 increased, and the otherwise beneficial commensal became an exacerbating factor during infection²⁵. We used CEent1 to examine the functional significance of the age-dependent *Enterobacteriaceae* bloom. Worms raised on CEent1 and shifted to *E. faecalis* at the end of larval development showed higher pathogen resistance compared to worms raised on the *E. coli* control, as previously shown. In contrast, worms raised on CEent1 to middle age before shifting to *E. faecalis* (day four of adulthood), midway through the *Enterobacteriaceae* bloom (Figs. 1 and 2), showed significantly lower pathogen resistance compared to worms raised on *E. coli* controls (Fig. 3A,B). Thus, the *Enterobacteriaceae* bloom has the potential to be detrimental to aging worms.

Changes in the intestinal niche associated with an age-dependent decline in DBL-1/BMP signaling may underlie the *Enterobacteriaceae* bloom

What may be the cause of the *Enterobacteriaceae* bloom? Experiments in microcosm environments and with defined communities showed that environmental availability was not a likely cause (Figs. 1B and 2A–D). Ecological succession, driven by the accumulating effects of interactions over time, also did not appear to contribute to the expansion (Fig. 1C). This was further supported by a comparison of CEent1-dsRed colonization in worms raised continuously, through larval development and into aging, on CEent1-dsRed monocultures versus worms shifted to CEent1-dsRed in different ages for a fixed duration of two days (see

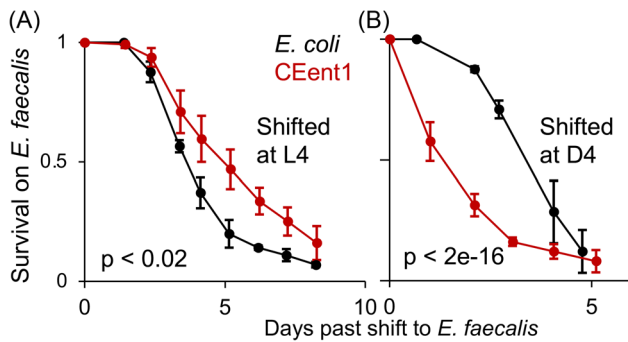


Figure 3. *Enterobacter hormaechei* CEent1 bloom in aging worms is associated with increased susceptibility to infection. Survival curves for wildtype (WT) worms raised on designated monocultures and shifted to plates with the pathogen, *E. faecalis*, (A) at L4 (n = 85–99/group) or (B) at day four of adulthood (n = 96–99). p values calculated with the log rank test.

Methods), which showed comparable age-dependent increases in *Enterobacteriaceae* abundance (Fig. 4A). We next examined whether an age-dependent decline in bacterial uptake may play a role in causing the bloom. To this end, we compared CEent1-dsRed colonization, as part of the SC20 community, in WT worms, which show an age-dependent decline in pharyngeal pumping (and thus bacterial uptake), and *eat-2* mutants, which lack a pharyngeal receptor for the neurotransmitter acetylcholine, resulting in a slow pumping rate, which does not change considerably during aging (Fig. 4B, inset). In both strains, we observed a similar course of age-dependent increases in CEent1-dsRed colonization (Fig. 4B), indicating that age-dependent changes in bacterial uptake likely did not contribute to the *Enterobacteriaceae* bloom.

DBL-1/BMP signaling is a conserved regulator of development, body size, and immunity⁵². Previous work identified a role for DBL-1-dependent immune regulation in shaping the worm gut microbiome, particularly affecting *Enterobacter* strains, which bloomed when genes encoding different components of this pathway were disrupted²⁵. Gene expression data in Wormbase (<https://wormbase.org>) suggested that expression of the pathway's components may decline at the end of larval development. To examine whether this indicated an age-dependent decline in

DBL-1 signaling and downstream gene expression, which might affect the gut microbiome, we used a transgenic worm strain expressing GFP from the *spp-9* promoter, previously shown to be negatively regulated by DBL-1 signaling²⁸. Fluorescent imaging demonstrated age-dependent increases in the expression of the GFP reporter, indicating a decline in DBL-1 signaling in aging worms (Fig. 5A). In agreement, the effects of either disruption or over-expression of the *dbl-1* ligand gene on GFP expression from the *spp-9* promoter diminished with age. The significance of *dbl-1* disruption was similarly lessened in aging worms for colonization with CEent1, which in middle-aged *dbl-1* mutants was comparable to that seen in WT animals, indicating a decline in DBL-1 signaling and in its involvement in controlling gut *Enterobacteriaceae* abundance during early aging (Fig. 5B). Additional experiments replicated the observation of the lessened importance of *dbl-1* disruption for CEent1 colonization as worms age (Fig. 5C, red box). These experiments also included *sma-4(syb2546)* mutants, which carry a *gof* mutation in DBL-1's transcriptional mediator and show a 20% increase in body length compared to WT animals (Fig. 5C, inset). *sma-4(gof)* mutants provided further support for a decline in DBL-1 control of gut bacteria, showing lower CEent1-dsRed colonization compared to WT animals in the early days of adulthood, increasing to WT levels by day 5 of adulthood (blue box compared to dotted line in Fig. 5C). While the effects of the *sma-4(gof)* mutation waned with age, not capable of restoring long-term control over CEent1 colonization, it was able to delay the CEent1 bloom. This had beneficial consequences, as *sma-4(gof)* mutants were partially protected from CEent1's detrimental effects on infection resistance in day four adults (Fig. 5D). Together, these results suggest that an age-dependent decline in DBL-1/BMP signaling alters the intestinal niche, permitting preferential accumulation of *Enterobacteriaceae*, which can be detrimental. Boosting DBL-1 signaling may mitigate the bloom and its consequences, but only partially.

Commensal communities can effectively mitigate the detrimental consequences of the *Enterobacteriaceae* bloom

The ability of the *sma-4(gof)* mutation to partially mitigate the detrimental effects of CEent1 expansion suggested that protection

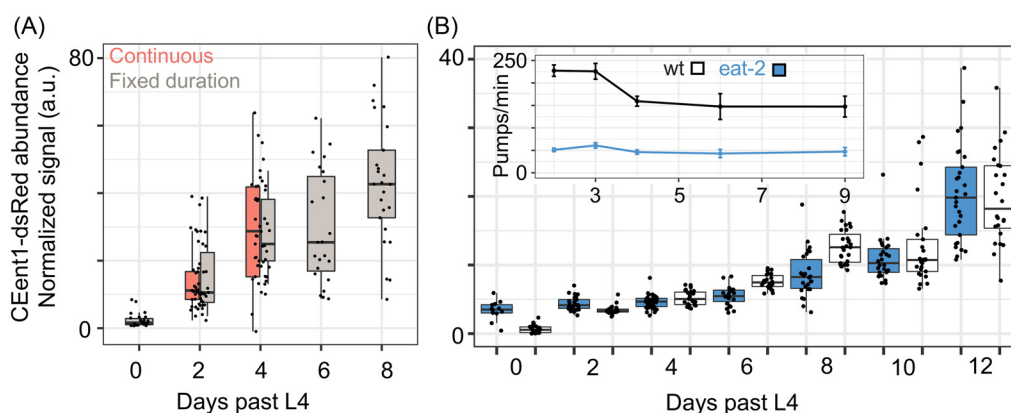


Figure 4. Neither the duration of exposure to bacteria nor the rate of uptake contributes to the *Enterobacteriaceae* bloom. (A) Colonization of aging worms by CEent1-dsRed following continuous exposure from larval stages or shifting worms for two days ending at the designated time points (fixed duration) (n = 22–27 worms/group/time point). Box and whisker plots show median values, marked with a line, with 25th and 75th percentile values delineating the box. (B) CEent1-dsRed colonization in WT and *eat-2* worms raised in the SC20 community (n = 10–36 worms/group/time point). Inset. Age-dependent declines in pumping rates (n = 4–10 worms/time point).

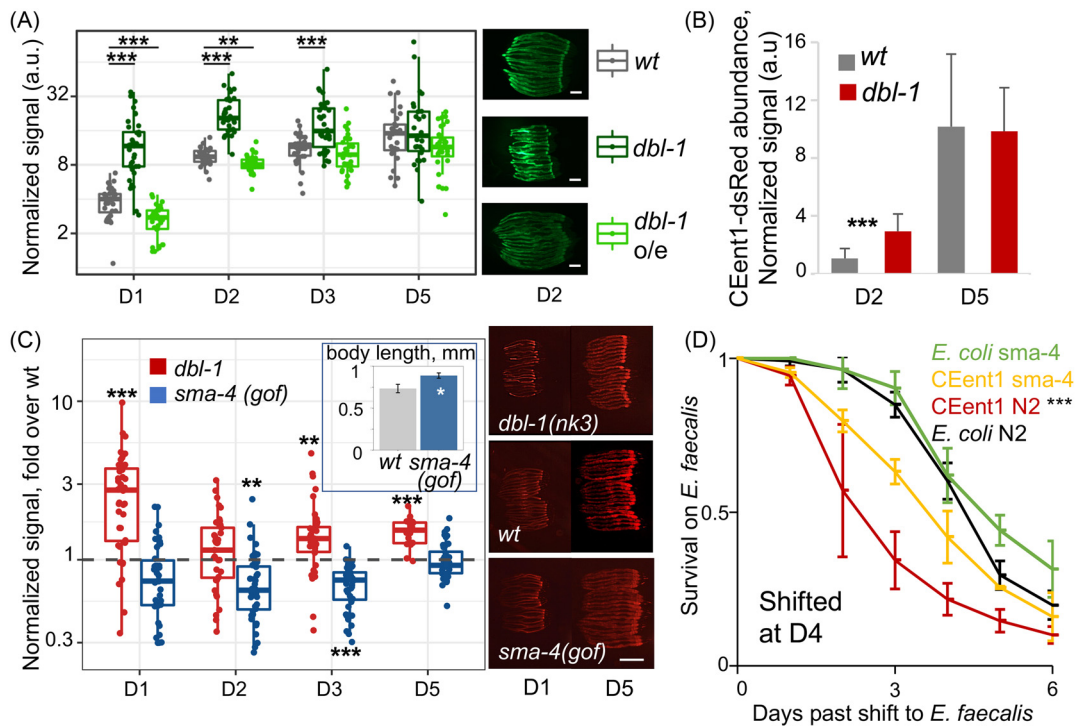


Figure 5. *Enterobacteriaceae* bloom is associated with an age-dependent decline in DBL-1/BMP signaling. (A) Green fluorescent protein expression from the *spp-9* promoter in designated strains; representative images (scale bar = 200 μ M) and quantification (n = 27–37/group/time point); **p < 0.01 and ***p < 0.001, Kruskal-Wallis rank sum test and post hoc Wilcoxon test (mutant vs. wt), Bonferroni corrected. (B) CEent1-dsRed colonization in worms of designated strains at designated days of adulthood; ***p < 0.001, t test. (C) Colonization of designated strains with CEent1-dsRed as part of CeMbio (n = 39–40/group/time point), quantified in images as those shown on the right (scale bar = 500 μ M) and presented as fold over wt median (dotted line). p values as in panel (A). **Inset.** Body length of young adult worms of designated strains measured using ImageJ (n = 9–12); *p < 0.0001, t test. (D) Survival of worms of designated strains raised on *E. coli* or CEent1 and shifted to *E. faecalis* at D4 of adulthood (n = 106–112/group); ***p < 0.001, log rank test, compared to worms raised on *E. coli*.

from an *Enterobacteriaceae* bloom is possible. Considering that the decline in DBL-1 signaling was also associated with an increased abundance of non-*Enterobacteriaceae* bacteria (Fig. 2), we examined whether other bacteria could compete with CEent1 and help prevent its detrimental effects. Recent work identified three members of the genus *Pantoea* as common *C. elegans* gut commensals that effectively colonize the worm gut and are capable of competing with an invading pathogen²³. WT worms raised on a community of the three commensals in addition to CEent1-dsRed (in equal parts) and shifted to *E. faecalis* in middle age (which with CEent1 alone would lead to compromised infection resistance), were as resistant as worms raised on *E. coli* alone and significantly more resistant than worms raised on a similar inoculum of CEent1-dsRed mixed with *E. coli* (Fig. 6A). While mortality on *E. faecalis* plates was attributed to the pathogen, 96.7% of the worms raised on the CEent1-dsRed/*E. coli* mix, which died in any of the days of the infection assay, were heavily colonized with CEent1-dsRed (Fig. 6A, inset), indicating proliferation alongside *E. faecalis*. In contrast, only 62.5% of the worms who were initially raised on the CEent1-dsRed/*Pantoea* mix were colonized, indicating that the *Pantoea* community was able to mitigate CEent1 proliferation in some of the worms and reduce mortality in the population.

To examine whether mitigating the detrimental effects of CEent1 proliferation was unique to *Pantoea*, worms were raised on a subset of seven members of CeMbio (see the Methods section), with or without BIGb0393 (one of the protective *Pantoea* strains, which is also a member of CeMbio), and with a large

excess of CEent1-dsRed (50% of total, to ensure effective colonization), and shifted at middle age to *E. faecalis*. Raising worms on the CeMbio subsets, with or without BIGb0393, conferred significantly higher resistance to infection than in worms raised on CEent1-dsRed alone (Fig. 6B). Again, fewer of the dead worms were colonized with CEent1-dsRed among those raised on CeMbio/CEent1-dsRed (51.4%), compared to those raised on CEent1-dsRed alone (84.6%). These experiments demonstrate that overproliferation of *Enterobacteriaceae* and its detrimental consequences in aging worms can be mitigated with more than one combination of gut commensals. Lastly, in the context of such a community, CEent1, or other *Enterobacteriaceae*, did not compromise the lifespan of their host, as worms grown on CeMbio with or without its *Enterobacteriaceae* members had a comparable lifespan (Fig. 6C).

Discussion

Our experiments identify an *Enterobacteriaceae* bloom as a hallmark of the gut microbiome in aging *C. elegans*. This bloom was observed in worms raised in natural-like microcosm environments with varying initial microbial diversity, as well as in worms raised on defined bacterial communities differing in the environmental availability of *Enterobacteriaceae*, indicating that it is independent of initial conditions. The *Enterobacteriaceae* bloom is not due to bacteria-driven ecological succession or to age-dependent changes in bacterial uptake. Rather, it is due to intrinsic age-dependent changes in the intestinal niche, suggesting that

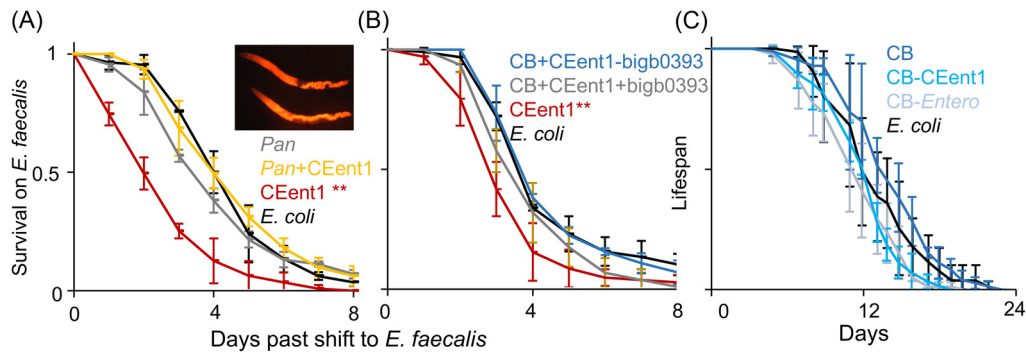


Figure 6. Commensal communities mitigate age-dependent susceptibility to infection. (A) Survival of worms raised on the designated strains/communities and shifted to *E. faecalis* at D4; Pan, a community of three *Pantoea* strains; ** $p < 0.0001$ (CEent1 compared to each group), log rank test ($n = 82\text{--}90$ /group); averages \pm SDs for three plate replicates. Inset. CEent1 colonized dead worms one day after shift to *E. faecalis*. (B) Survival of worms raised on a designated subset of CeMbio (CB) and shifted to *E. faecalis* at D4; BIGb0393, a *Pantoea* strain ** $p < 0.0001$ ($n = 95\text{--}105$ /group). Shown are the results of one representative experiment out of two with similar results. (C) Lifespan of WT worms raised in designated communities. Entero stands for *Lelliottia* Jub66 and *Enterobacter* CEent1. Averages \pm SDs for three plate replicates ($n = 67\text{--}79$ /group).

the bloom is a signature of chronological age. Our results demonstrate that an increased gut abundance of *Enterobacteriaceae* strains may have detrimental consequences for aging animals, at least for infection resistance. However, in the context of a community, even with restricted diversity, the detrimental consequences of this bloom can be mitigated. Our results highlight the *Enterobacteriaceae* bloom as a hallmark of chronological aging but suggest that the consequences of this bloom are context-dependent, with microbiome composition representing the context that can differentiate between healthy and unhealthy aging.

It is accepted that aging is accompanied by gut dysbiosis^{7–9,14,53}. Human studies have documented diverse changes in gut microbiome composition. Among those, increased abundance of *Proteobacteria/Pseudomonadota*, and specifically of *Enterobacteriaceae*, is a recurring theme^{17,54}. In line with this, our results show a replicable age-associated expansion of *Enterobacteriaceae*, suggesting that it may be an evolutionarily conserved signature of aging. What causes this bloom is not clear. A study in fruit flies described gut dysbiosis as characterized by a biphasic change in the microbiome of aging flies, in which a midlife bloom of *g-proteobacteria* led to intestinal barrier dysfunction and a subsequent increase in *a-proteobacteria*⁷. While barrier dysfunction was suggested as the cause of gut dysbiosis⁵⁵, what initiated the *g-proteobacteria* bloom was not clear. The *Enterobacteriaceae* bloom we observed in worms may be analogous to the initial phase of dysbiosis in flies. In worms, the initiation of the *Enterobacteriaceae* bloom was associated with a decline in DBL-1/BMP signaling. DBL-1 signaling was previously shown to play a central role in controlling gut *Enterobacteriaceae*²⁵. Thus, its age-dependent decline may change the host intestinal niche, making it more permissive for *Enterobacteriaceae* expansion. Supporting a causal role for DBL-1 signaling in the *Enterobacteriaceae* bloom, *gof* mutants for the SMA-4 BMP mediator showed a delay in *Enterobacter* colonization as well as attenuated infection susceptibility. These results suggest that the decline of immune signaling during aging is an important factor in initiating dysbiosis. However, at least in the case of SMA-4, revamping the immune pathway to mitigate the detrimental effects of the bloom was only partially successful, suggesting that additional changes in the gut niche may take place to promote the *Enterobacteriaceae* bloom and further limiting the potential of DBL-1/BMP reactivation in aging worms as an intervention to alleviate gut dysbiosis.

Enterobacteriaceae blooms are associated with increased susceptibility to infection^{56–59}. In agreement with this, the expansion of *E. hormaechei* CEent1 in aging worms compromised infection resistance and survival. Continued gut accumulation of CEent1 following a shift to pathogen plates further suggests that in old worms, CEent1 (and perhaps additional *Enterobacteriaceae* members) was an opportunistic pathogen, or a pathobiont. Previous results support the notion that CEent1 was a pathobiont, as worms growing on CEent1 alone have a shorter lifespan compared to those raised on an *E. coli* diet²². However, in the context of a community (CeMbio), inclusion or removal of CEent1 did not have any effect on lifespan, supporting the importance of a diverse microbiome in keeping pathobionts in check as the host ages.

Conclusions

The genetic tractability and short lifespan of *C. elegans* have made it a useful model for aging research. Its more recent establishment as a model for microbiome research adds to the advantages of longitudinal microbiome analysis in clonal host populations, while having greater control over bacterial availability, to facilitate studies of host-microbiome interactions during aging. Using this model, we identified what seems to be an evolutionary conserved signature of dysbiosis in aging animals and have begun to dissect its causes as well as its consequences. As is often seen in different scenarios of gut dysbiosis, the *Enterobacteriaceae* bloom that we identified is associated with pathology. However, this pathology can be circumvented by manipulating the gut microbiome using various commensal communities. Thus, while an *Enterobacteriaceae* bloom seems to be an inevitable consequence of aging, its extent and outcomes can be restrained by other members of the gut microbiome. What differentiates between communities that can or cannot achieve this remains to be seen.

Acknowledgments

We thank Dr. Heidi Goodrich-Blaire for providing the plasmids required for constructing the dsRed-expressing *Enterobacter hormaechei*, Dr. Tina Gumienny for *spp-9* reporter strains, and Dr. Andrew Dillin for *eat-2* mutants.

Funding

The work described in this article was supported by NIH grants R01OD024780, R01AG061302 (M.S.), and R21AG075315 (C.S.-D.). D.K. was supported by NSF fellowship DGE 2146752. J.C. was supported by a fellowship from Berkeley's Center for Research in Aging.

Authors' Contributions

R.C., M.B., and M.S. conceived the project, and M.S. supervised it; M.B. conducted microcosm experiments, which were analyzed by D.K., R.C., R.B., B.P., D.M., E.D., and J.C. carried out experiments and analyses. V.N. generated the CEent1-dsRed strain. C.S.-D. designed the *sma-4* *gof* strain, characterized its function, and helped with writing the article. R.C. and M.S. compiled the results and wrote the article.

Availability of Data and Materials

Raw 16S rRNA gene sequencing data and metadata can be accessed at <https://www.ncbi.nlm.nih.gov/sra> with accession number PRJNA982115.

Supplementary Materials

Supplemental information can be found online at <https://doi.org/10.59368/agingbio.20240024>.

Accepted January 22, 2024

Published March 15, 2024

References

- Nicholson J.K., Holmes E., Kinross J., Burcelin R., Gibson G., Jia W., & Pettersson S. (2012). Host-gut microbiota metabolic interactions. *Science* **336**(6086), 1262–1267. PMID: 22674330; doi: 10.1126/science.1223813.
- Dominguez-Bello M.G., Godoy-Vitorino F., Knight R., & Blaser M.J. (2019). Role of the microbiome in human development. *Gut* **68**(6), 1108–1114. PMID: 30670574; doi: 10.1136/gutjnl-2018-317503.
- Fan Y., & Pedersen O. (2021). Gut microbiota in human metabolic health and disease. *Nat. Rev. Microbiol.* **19**(1), 55–71. PMID: 32887946; doi: 10.1038/s41579-020-0433-9.
- Morais L.H., Schreiber H.L., & Mazmanian S.K. (2021). The gut microbiota–brain axis in behaviour and brain disorders. *Nat. Rev. Microbiol.* **19**(4), 241–255. PMID: 33093662; doi: 10.1038/s41579-020-00460-0.
- Turnbaugh P.J., Backhed F., Fulton L., & Gordon J.I. (2008). Diet-induced obesity is linked to marked but reversible alterations in the mouse distal gut microbiome. *Cell Host Microbe* **3**(4), 213–223. PMID: 18407065; doi: 10.1016/j.chom.2008.02.015.
- Mariño E., Richards J.L., McLeod K.H., Stanley D., Yap Y.A., Knight J., ... Mackay C.R. (2017). Gut microbial metabolites limit the frequency of autoimmune T cells and protect against type 1 diabetes. *Nat. Immunol.* **18**(5), 552–562. PMID: 28346408; doi: 10.1038/ni.3713.
- Clark R.I., Salazar A., Yamada R., Fitz-Gibbon S., Morselli M., Alcaraz J., ... Walker D.W. (2015). Distinct shifts in microbiota composition during drosophila aging impair intestinal function and drive mortality. *Cell Rep.* **12**(10), 1656–1667. PMID: 26321641; doi: 10.1016/j.celrep.2015.08.004.
- O'Toole P.W., & Jeffery I.B. (2015). Gut microbiota and aging. *Science* **350**(6265), 1214–1215. PMID: 26785481; doi: 10.1126/science.aac8469.
- Thevaranjan N., Puchta A., Schulz C., Naidoo A., Szamosi J.C., Verschoor C.P., ... Bowdish D.M.E. (2017). Age-associated microbial dysbiosis promotes intestinal permeability, systemic inflammation, and macrophage dysfunction. *Cell Host Microbe* **21**(4), 455–466.e4. PMID: 28407483; doi: 10.1016/j.chom.2017.03.002.
- Wilmanski T., Diener C., Rappaport N., Patwardhan S., Wiedrick J., Lapidus J., ... Price N.D. (2021). Gut microbiome pattern reflects healthy ageing and predicts survival in humans. *Nat. Metab.* **3**(2), 274–286. PMID: 33619379; doi: 10.1038/s42255-021-00348-0.
- Biagi E., Franceschi C., Rampelli S., Severgnini M., Ostan R., Turroni S., ... Candela M. (2016). Gut microbiota and extreme longevity. *Curr. Biol.* **26**(11), 1480–1485. PMID: 27185560; doi: 10.1016/j.cub.2016.04.016.
- Kim K.H., Chung Y., Huh J.-W., Park D.J., Cho Y., Oh Y., ... Kim J.F. (2022). Gut microbiota of the young ameliorates physical fitness of the aged in mice. *Microbiome* **10**(1), 238. PMID: 36567320; doi: 10.1186/s40168-022-01386-w.
- Parker A., Romano S., Ansoorge R., Aboelnour A., Le Gall G., Savva G.M., ... Carding S.R. (2022). Fecal microbiota transfer between young and aged mice reverses hallmarks of the aging gut, eye, and brain. *Microbiome* **10**(1), 68. PMID: 35501923; doi: 10.1186/s40168-022-01243-w.
- Smith P., Willemsen D., Popkes M., Metge F., Gandiwa E., Reichard M., & Valenzano D.R. (2017). Regulation of life span by the gut microbiota in the short-lived African turquoise killifish. *eLife* **6**, e27014. PMID: 28826469; doi: 10.7554/eLife.27014.
- Bárcena C., Valdés-Mas R., Mayoral P., Garabaya C., Durand S., Rodríguez F., ... López-Otín C. (2019). Healthspan and lifespan extension by fecal microbiota transplantation into progeroid mice. *Nat. Med.* **25**(8), 1234–1242. PMID: 31332389; doi: 10.1038/s41591-019-0504-5.
- Adriansjach J., Baum S.T., Lefkowitz E.J., Van Der Pol W.J., Buford T.W., & Colman R.J. (2020). Age-related differences in the gut microbiome of rhesus macaques. *J. Gerontol. Ser. A* **75**(7), 1293–1298. PMID: 32052009; doi: 10.1093/gerona/glaa048.
- Leite G., Pimentel M., Barlow G.M., Chang C., Hosseini A., Wang J., ... Mathur R. (2021). Age and the aging process significantly alter the small bowel microbiome. *Cell Rep.* **36**(13), 109765. PMID: 34592155; doi: 10.1016/j.celrep.2021.109765.
- Shapira M. (2017). Host–microbiota interactions in *Caenorhabditis elegans* and their significance. *Curr. Opin. Microbiol.* **38**, 142–147. PMID: 28623729; doi: 10.1016/j.mib.2017.05.012.
- Berg M., Stenuit B., Ho J., Wang A., Parke C., Knight M., ... Shapira M. (2016). Assembly of the *Caenorhabditis elegans* gut microbiota from diverse soil microbial environments. *ISME J.* **10**(8), 1998–2009. PMID: 26800234; doi: 10.1038/ismej.2015.253.
- Dirksen P., Marsh S.A., Braker I., Heitland N., Wagner S., Nakad R., ... Schulenburg H. (2016). The native microbiome of the nematode *Caenorhabditis elegans*: Gateway to a new host-microbiome model. *BMC Biol.* **14**(1), 38. PMID: 27160191; doi: 10.1186/s12915-016-0258-1.
- Zhang F., Berg M., Dierking K., Félix M.-A., Shapira M., Samuel B.S., & Schulenburg H. (2017). *Caenorhabditis elegans* as a model for microbiome research. *Front. Microbiol.* **8**. PMID: 28386252; doi: 10.3389/fmicb.2017.00485.
- Berg M., Zhou X.Y., & Shapira M. (2016). Host-specific functional significance of *Caenorhabditis* gut commensals. *Front. Microbiol.* **7**. PMID: 27799924; doi: 10.3389/fmicb.2016.01622.
- Pérez-Carrascal O.M., Choi R., Massot M., Pees B., Narayan V., & Shapira M. (2022). Host preference of beneficial commensals in a microbially-diverse environment. *Front. Cell Infect. Microbiol.* **12**. PMID: 35782135; doi: 10.3389/fcimb.2022.795343.
- Slowinski S., Ramirez I., Narayan V., Somayaji M., Para M., Pi S., ... Shapira M. (2020). Interactions with a complex microbiota mediate a trade-off between the host development rate and heat stress resistance. *Microorganisms* **8**(11), 1781. PMID: 33202910; doi: 10.3390/microorganisms8111781.
- Berg M., Monnin D., Cho J., Nelson L., Crits-Christoph A., & Shapira M. (2019). TGF β /BMP immune signaling affects abundance and function of *C. elegans* gut commensals. *Nat. Commun.* **10**, 1–12. PMID: 30723205; doi: 10.1038/s41467-019-08379-8.
- Taylor M., & Vega N.M. (n.d.). Host immunity alters community ecology and stability of the microbiome in a *Caenorhabditis elegans* model. *mSystems* **6**, e00608-20. PMID: 33879498; doi: 10.1128/mSystems.00608-20.

27. Zhang F., Weckhorst J.L., Assié A., Hosea C., Ayoub C.A., Khodakova A.S., ... Samuel B.S. (2021). Natural genetic variation drives microbiome selection in the *Caenorhabditis elegans* gut. *Curr. Biol.* **31**(12), 2603–2618.e9. PMID: 34048707; doi: 10.1016/j.cub.2021.04.046.
28. Lakdawala M.F., Madhu B., Faure L., Vora M., Padgett R.W., & Gumienny T.L. (2019). Genetic interactions between the DBL-1/BMP-like pathway and dpy body size-associated genes in *Caenorhabditis elegans*. *Mol. Biol. Cell* **30**(26), 3151–3160. PMID: 31693440; doi: 10.1091/mbc.E19-09-0500.
29. Madhu B., Lakdawala M.F., Issac N.G., & Gumienny T.L. (2020). *Caenorhabditis elegans* saposin-like spp-9 is involved in specific innate immune responses. *Genes Immun.* **21**(5), 301–310. PMID: 32770079; doi: 10.1038/s41435-020-0108-6.
30. Wu J.-W., Hu M., Chai J., Seoane J., Huse M., Li C., ... Shi Y. (2001). Crystal structure of a phosphorylated Smad2: Recognition of phosphoserine by the MH2 domain and insights on Smad function in TGF- β signaling. *Mol. Cell* **8**(6), 1277–1289. PMID: 11779503; doi: 10.1016/S1097-2765(01)00421-X.
31. Wang J., Tokarz R., & Savage-Dunn C. (2002). The expression of TGF β signal transducers in the hypodermis regulates body size in *C. elegans*. *Development* **129**(21), 4989–4998. PMID: 12397107; doi: 10.1242/dev.129.21.4989.
32. Hata A., Lo R.S., Wotton D., Lagna G., & Massagué J. (1997). Mutations increasing autoinhibition inactivate tumour suppressors Smad2 and Smad4. *Nature* **388**(6637), 82–87. PMID: 9214507; doi: 10.1038/40424.
33. Dirksen P., Assié A., Zimmermann J., Zhang F., Tietje A.-M., Marsh S.A., ... Samuel B.S. (2020). CeMbio - The *Caenorhabditis elegans* microbiome resource. *G3: Genes, Genomes, Genet.* **10**(9), 3025–3039. PMID: 32669368; doi: 10.1534/g3.120.401309.
34. McKown R.L., Waddell C.S., Arciszewska L.K., & Craig N.L. (1987). Identification of a transposon Tn7-dependent DNA-binding activity that recognizes the ends of Tn7. *Proc. Natl. Acad. Sci. U. S. A.* **84**(22), 7807–7811. PMID: 2825163; doi: 10.1073/pnas.84.22.7807.
35. Teal T.K., Lies D.P., Wold B.J., & Newman D.K. (2006). Spatiotemporal stratification of *Shewanella oneidensis* biofilms. *Appl. Environ. Microbiol.* **72**(11), 7324–7330. PMID: 16936048; doi: 10.1128/AEM.01163-06.
36. Murfin K.E., Chaston J., & Goodrich-Blair H. (2012). Visualizing bacteria in nematodes using fluorescent microscopy. *J. Vis. Exp.* PMID: 23117838; doi: 10.3791/4298.
37. Bao Y., Lies D.P., Fu H., & Roberts G.P. (1991). An improved Tn7-based system for the single-copy insertion of cloned genes into chromosomes of gram-negative bacteria. *Gene* **109**(1), 167–168. PMID: 1661697; doi: 10.1016/0378-1119(91)90604-A.
38. Trang K., Bodkhe R., & Shapira M. (2022). Compost microcosms as microbially diverse, natural-like environments for microbiome research in *Caenorhabditis elegans*. *J. Vis. Exp. JoVE.* PMID: 36190292; doi: 10.3791/64393.
39. Shapira M., & Tan M.-W. (2008). Genetic analysis of *caenorhabditis elegans* innate immunity. In: Ewbank J. and Vivier E., eds. *Innate Immunity*. Totowa, NJ: Humana Press: 429–442.
40. Bolyen E., Rideout J.R., Dillon M.R., Bokulich N.A., Abnet C.C., Al-Ghalith G.A., ... Caporaso J.G. (2019). Reproducible, interactive, scalable and extensible microbiome data science using QIIME 2. *Nat. Biotechnol.* **37**(8), 852–857. PMID: 31341288; doi: 10.1038/s41587-019-0209-9.
41. Edgar R.C. (2010). Search and clustering orders of magnitude faster than BLAST. *Bioinforma. Oxf. Engl.* **26**(19), 2460–2461. PMID: 20709691; doi: 10.1093/bioinformatics/btq461.
42. Faith D.P. (1994). Genetic diversity and taxonomic priorities for conservation. *Biol. Conserv.* **68**(1), 69–74. doi: 10.1016/0006-3207(94)90548-7.
43. Shannon C.E. (1997). The mathematical theory of communication. *MD Comput. Comput. Med. Pract.* **14**, 306–317. PMID: 9230594.
44. Schindelin J., Arganda-Carreras I., Frise E., Kaynig V., Longair M., Pietzsch T., ... Cardona A. (1963). Fiji: An open-source platform for biological-image analysis. *Nat. Methods* **9**(7), 676–682. PMID: 22743772; doi: 10.1038/nmeth.2019.
45. Livak K.J., & Schmittgen T.D. (2001). Analysis of relative gene expression data using real-time quantitative PCR and the 2- $\Delta\Delta$ CT method. *Methods.* PMID: 11846609; doi: 10.1006/meth.2001.1262.
46. Shapira M., Hamlin B.J., Rong J., Chen K., Ronen M., & Tan M.-W. (2012). A conserved role for a GATA transcription factor in regulating epithelial innate immune responses. *Proc. Natl. Acad. Sci. U. S. A.* **103**(38), 14086–14091. PMID: 16968778; doi: 10.1073/pnas.0603424103.
47. Garsin D.A., Sifri C.D., Mylonakis E., Qin X., Singh K.V., Murray B.E., ... Ausubel F.M. (2006). A simple model host for identifying gram-positive virulence factors. *Proc. Natl. Acad. Sci. U. S. A.* **98**(19), 10892–10897. PMID: 11535834; doi: 10.1073/pnas.191378698.
48. Sifri C.D., Mylonakis E., Singh K.V., Qin X., Garsin D.A., Murray B.E., ... Calderwood S.B. (2001). Virulence Effect of *Enterococcus faecalis* protease genes and the quorum-sensing locus *fsr* in *Caenorhabditis elegans* and mice. *Infect. Immun.* **70**(10), 5647–5650. PMID: 12228293; doi: 10.1128/IAI.70.10.5647-5650.2002.
49. Therneau T.M., Lumley T., Elizabeth A., & Cynthia C. (2023). Survival: Survival analysis 2023. <https://CRAN.R-project.org/package=survival>.
50. Villanueva R.A.M., & Chen Z.J. (2019). ggplot2: Elegant graphics for data analysis (2nd ed.). *Meas. Interdiscip. Res. Perspect.* **17**(3), 160–167. doi: 10.1080/15366367.2019.1565254.
51. Langille M.G., Meehan C.J., Koenig J.E., Dhanani A.S., Rose R.A., Howlett S.E., & Beiko R.G. (2014). Microbial shifts in the aging mouse gut. *Microbiome* **2**(1), 50. PMID: 25520805; doi: 10.1186/s40168-014-0050-9.
52. Savage-Dunn C., & Padgett R.W. (2017). The TGF- β family in *Caenorhabditis elegans*. *Cold Spring Harb. Perspect Biol.* **9**(6), a022178. PMID: 28096268; doi: 10.1101/cshperspect.a022178.
53. Claesson M.J., Cusack S., O'Sullivan O., Greene-Diniz R., de Weerd H., Flannery E., ... O'Toole P.W. (2011). Composition, variability, and temporal stability of the intestinal microbiota of the elderly. *Proc. Natl. Acad. Sci. U. S. A.* **108**, 4586–4591. PMID: 20571116; doi: 10.1073/pnas.1000097107.
54. Odamaki T., Kato K., Sugahara H., Hashikura N., Takahashi S., Xiao J., ... Osawa R. (2016). Age-related changes in gut microbiota composition from newborn to centenarian: a cross-sectional study. *BMC Microbiol.* **16**(1), 90. PMID: 27220822; doi: 10.1186/s12866-016-0708-5.
55. Salazar A.M., Resnik-Docampo M., Ulgherait M., Clark R.I., Shirasu-Hiza M., Jones D.L., & Walker D.W. (2018). Intestinal Snakeskin limits microbial dysbiosis during aging and promotes longevity. *iScience* **9**, 229–243. PMID: 30419503; doi: 10.1016/j.isci.2018.10.022.
56. Lupp C., Robertson M.L., Wickham M.E., Sekirov I., Champion O.L., Gaynor E.C., & Finlay B.B. (2007). Host-mediated inflammation disrupts the intestinal microbiota and promotes the overgrowth of Enterobacteriaceae. *Cell Host Microbe* **2**(2), 119–129. PMID: 18005726; doi: 10.1016/j.chom.2007.06.010.
57. Bailey M.T., Dowd S.E., Parry N.M.A., Galley J.D., Schauer D.B., & Lyte M. (2010). Stressor exposure disrupts commensal microbial populations in the intestines and leads to increased colonization by *Citrobacter rodentium*. *Infect. Immun.* **78**(4), 1509–1519. PMID: 20145094; doi: 10.1128/IAI.00862-09.
58. Shaler C.R., Parco A.A., Elhenawy W., Dourka J., Jury J., Verdu E.F., & Coombes B.K. (2021). Psychological stress impairs IL22-driven protective gut mucosal immunity against colonising pathobionts. *Nat. Commun.* **12**(1), 6664. PMID: 34795263; doi: 10.1038/s41467-021-26992-4.
59. Schlechte J., Zucoloto A.Z., Yu I., Doig C.J., Dunbar M.J., McCoy K.D., & McDonald B. (2023). Dysbiosis of a microbiota-immune metasytem in critical illness is associated with nosocomial infections. *Nat. Med.* **29**(4), 1017–1027. PMID: 36894652; doi: 10.1038/s41591-023-02243-5.